Development of a MATLAB-based code for quantification of effective void space in porous pavement

Rebecca Allen[a,*], Berthe Dongmo-Engeland[a], Saja Al-Bata[a]

[a]*Department of Built Environment, Oslo Metropolitan University, Norway*
[*]rebeccaa@oslomet.no

Abstract

Porous pavement is a well-documented, low-impact stormwater management technique. When it comes to design of the top layer, the amount of void space (porosity) is often of interest as it influences both infiltration and strength of the pavement. Laboratory equipment can be used to measure the porosity of core samples, but when more detail is required, other equipment or methods must be used. One such method is to scan the entire sample using a computer tomography (CT) machine and then perform some image processing techniques on the scanned data to reconstruct the sample digitally. While the workflow of scanning and processing to produce the 3D digital twin of porous pavement is not new and can be in fact done by open-source or commercial software, there are still some parts of the process that deserve a deeper investigation, for example binarization and segmentation algorithms applied to the solid-and-void space and void space, respectively. This is difficult to do with commercial software which operates like a black-box, and there needs to be more open-source codes that are user-friendly, extendable, and competitive to what commercial software can do. This work presents a MATLAB-based code that allows for a deeper investigation of how one can accurately and efficiently quantify the effective (or connected) void space of a porous pavement sample from a 3D digital model. We demonstrate the effect of dataset coarsening, which can be used to reduce the computational intensity of the algorithm while preserving accuracy. The code is publicly available online to allow for reproducible research and the possibility of extensions for increased functionality and complexity.

1. Introduction

Asphalt is ubiquitous in city parking lots, roads and highways, and research is often focused on how to increase its lifespan to minimize maintenance costs. However, one problem that arises with asphalt covered surfaces is storm water management: excessive rainfall leads to high volumes of runoff that must be managed properly to avoid surface flooding. Traditional methods to handle this surface flooding involve collecting runoff in storm sewers and moving this water either directly to a body of water (lake or sea) or to an area where it can collect before eventually draining into the ground.

An alternative approach to stormwater management involves the use of asphalt which is typically termed *porous* asphalt (PA) or also *drainage* asphalt (DA) (Dylla & Hansen, 2015), and is typically recommended for parking areas and low-volume roadways (Roseen et al., 2012). As these names imply, the role of this alternative asphalt is to allow surface water to permeate through the layer, from top to bottom, while at the same time remaining strong enough to sustain typical vehicle loads. The challenge is thus the trade-off between a higher-than-typical porosity and reduced strength. When installed as an overlay above traditional impervious asphalt pavements, PA is known as Permeable (or Porous) Friction Course (PFC), Porous European Mix (PEM) or Open-Graded Friction Course (OGFC), a type of pavement developed to improve road safety under wet conditions and reduce noise (Stanard et al., 2007; Watson et al., 2018). Noise reduction and improved safety are the reason why the surface layer of the majority (>90%) of the Dutch principal motorway network consists of a course PA (Aalst et al., 2015; Bondt et al., 2016; Plug & Bondt, 2021).

Advances in PA research can be realized through studying the unique relationship between porosity and strength. Studies (Chen et al., 2021, Ferreira et al., 2021, Król et al., 2017) have focused on obtaining empirically-derived expressions for permeability as a function of porosity. The value of these expressions lies in the fact that they can be used to predict permeability given a certain change in porosity caused by clogging, for example. But first, to capture the PA's ability to filter water, the

connected[1] pore space needs to be determined, i.e., the amount of the total pore space that becomes filled with water as it flows from top to bottom of the layer. The other pore space can be classified as *isolated* since they are not directly connected to the connected pores. Determining the total volume of the connected pore space can be measured in a lab with the right equipment, however information about the exact geometry of the connected pore space is required in order to study the infiltrating- or permeable-behavior of the PA. A popular and non-destructive method to get highly-resolved pore space details involves taking hundreds of 2D images of a PA sample using a computer-tomography (CT) scanner and then performing a set of image processing techniques on these 2D images to construct a 3D digital representation of the sample (Schuck et al. 2021). This same workflow of imaging, processing, and 3D reconstruction of a so-called *digital twin* has also been applied to many other areas of application, such as pervious concrete (Jagadeesh et al., 2022), geomaterials (Quinteros & Carraro, 2023), and even green roofs (De-Ville et al., 2017).

The studies cited above involve independent efforts at preforming image processing techniques in order to extract meaningful information from the CT-scan images. Some use commercial software (Simpleware ScanIP, Avizo) while others develop their own programs or codes that rely on either open-source programming languages and their image-processing tools (Python-based Spam) or license-based programming languages and their image processing tools (MATLAB-based Image Processing Toolbox). While commercial software certainly has its strengths – it is validated, robust, developed by a team of people, and hopefully user-friendly – the efforts of developing a computer program or code to perform research on PA is also valuable and arguably more flexible and *open* than its commercial software competitors. And yet, even though we have found several studies that are based on self-generated code, we find a lack of reproducibility in the research community when it comes to image segmentation applied on PA samples and algorithms used to extract the effective pore space. For example, Schuck et al., 2021 and Jagadeesh et al., 2022 documented very clearly their image processing steps, however leave the reader without any code that could be applied to their work. We understand that it is not always the objective of a researcher to openly publish their developed programs and codes, however we see the benefit that code-sharing can have in the research community. As such, a main objective of this work is to start an online repository (find link at end of paper), for porous media characterization beginning with asphalt samples. Specifically, this study focuses on processing a stack of micro-CT images of asphalt using built-in MATLAB functions and on the characterization of the sample according to its local and global porosity. The code is applied on images from two sources: a laboratory made PA sample and a cored sample from a county road in Norway. The cored sample is not a PA sample but rather considered as regular asphalt and is used to demonstrate the code's ability to quantity porosity in samples with very low porosity.

2. Materials and Methodology

2.1. Asphalt Samples

The asphalt samples studied in this work are shown in Figure 1. "DA" stands for drainage asphalt[2], and "H" stands for Hafjell, a location in Norway where the sample was extracted. The photo for sample 1H is in fact a photo of sample 3H (both of which are studied in Kassem et al., 2023), however it is presented here as a representative photo since they were both cut from the same road. Material details of the DA and 1H samples are summarized in Table 1. The binder type was regular (PGB) for the DA sample and modified with polymer (PMB) for the 1H sample. Dmax stands for the maximum aggregate size.

Figure 1: The porous (left) and regular asphalt (right) samples considered in this work.

Table 1: Material information of samples.

Spec. \ Sample	DA 11 A	1H
Type	Porous	Regular
Source	Lab-made	Cored
Binder type	PGB 70/100	PMB 65/105-60
Dmax	11	16

[1] Some researchers use the term *connected* while some use the term *effective*.

[2] PA (porous asphalt) and DA (drainage asphalt) are used interchangeably in this work.

2.2. Computer Tomography (CT) Scanning

Scanning of the samples was done at the Norwegian Geotechnical Institute (NGI) in Oslo, using a Nikon Metrology XT H-225LC device. Details of the scans are summarized in Table 2. Two-thousand projections were used for the DA sample which means a total of 2000 .tiff images were created and each image contained 2000 by 2000 pixels. However, the sample itself and its volume of interest (VOI) take up only a portion of the images; the number of pixels in the 2D region of interest (ROI) and the number of images that make up the VOI are reported in Table 2, and the total number of voxels is the product of these two. As such, the total number of cells in the VOI is less than $(2000)^3$.

Table 2: CT image specifications and dataset sizes in terms of ROI (region of interest) and VOI (volume of interest).

Spec. / Sample	DA	1H
Voxel size (µm)	62.6	56.3
# of projections	2000	2500
# pixels in ROI	1.87×10^6	2.25×10^6
# images in VOI	901	701
# voxels in VOI	1.68×10^9	1.57×10^9

2.3. Image Processing

The CT scanning procedure produced hundreds of .tiff files for each sample, with a total size of 7.5 and 6 Gigabytes for the DA sample and the regular sample, respectively. These image files were processed using MATLAB release version R2021a, MATLAB's Image Processing Toolbox, and a laptop with Intel(R) i7-1165G7@2.8Hz CPU and 32 GB memory. The basic steps taken to process these image files with the objective of detecting the connected pore space is summarized below:

1. Read each .tiff 2D image file
2. Define a ROI, applied to each image
3. Crop and mask the image data to the ROI
4. Filter out noise from each image with either a median filter and/or a Gaussian filter
5. Detect total pore space in each 2D image using a binarization method, based on either automatic or manual thresholding
6. Construct the 3D volume of total pore space by assembling stack of the 2D total pore spaces
7. Apply the *detect-connected-pores* algorithm on total pore volume to detect the top-to-bottom connected pore volume

The region of interest (ROI) was manually cropped with a draw circle tool such that all the space beyond the sample boundaries, in addition to a small outer ring of sample, was labelled as outside the ROI. This ensured we were focusing only on the sample. The noise reduction filters used were a median filter followed by a Gaussian (with standard deviation equal to 2) for the PA sample and Gaussian (with standard deviation equal to 2) followed by adaptive histogram equalization for the 1H sample. The binarization method was based on manual thresholding for both samples. The output of steps 1 to 5 are presented in Figure 2, and output from steps 6 to 7 in Figure 3.

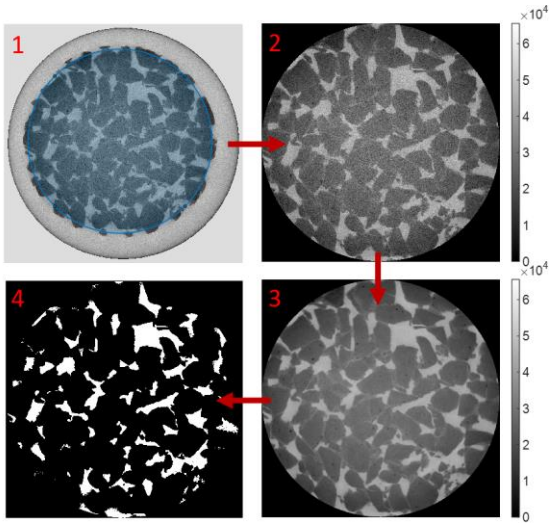

Figure 2: Visualization of the various stages of image processing, from 1-original, 2-cropped and masked, 3-filtered, and 4-binarized image.

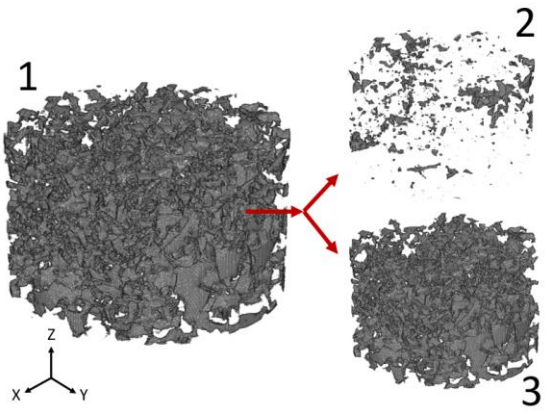

Figure 3: Visualization of a constructed 3D pore volume (1) which is made up of isolated pores (2) and connected pores (3).

2.4. Detecting Connected Pores

The main contribution of this work is the detect-connected-pores algorithm which is openly available online (find link at end of paper). The basic idea of the algorithm is to initialize and continually update a pore cell map, which includes the index of all the pore cells as well as the indices of the 6 neighboring cells. Besides the index, a label is assigned to each pore cells (2=pore needs checking, 1=connected pore). All pore cells in the

top image are immediately labelled with as a top-connected pore. Then a while-loop is used to continually update the labelling of the pore cells based on whether or not they have a neighboring cell that is labelled as top-connected. To help with performance, the neighboring cells that were just used to label a pore cell as top-connected is labelled with NaN so they are skipped over during any consecutive iterations. Two while-loops are required: the first one detects all top-connected pore cells, and the second one detects all bottom-connected pore cells. Two while-loops are used because a pore cell could be connected to other pore cells that eventually lead up to the top of the sample. However, this does not mean they will lead down to the bottom of the sample. Thus, the top-to-bottom connected pores are pores which are common to both the top-connected AND bottom-connected pathways.

3. Results

We present total pore space results for each sample (DA and 1H), since the 1H sample provides a nice comparison to a regular and road-cut asphalt sample. However, afterwards we focus our attention on the DA sample only since the 1H sample lacks a "top-to-bottom" connected pore space.

The connected pore space that was extracted using the detect-connected-pores algorithm on the DA sample is illustrated on the left side of Figure 4. The right side of Figure 4 illustrates all the pore space of sample 1H because a top-to-bottom connected pore space could not be detected in this sample. This is not surprising given that it was not designed to infiltrate water.

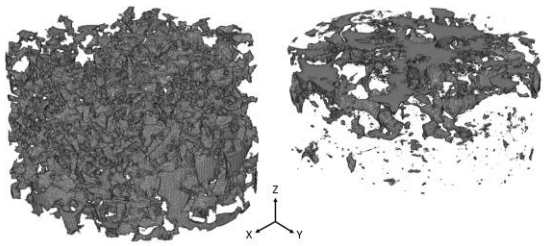

Figure 4: Connected pore space in our DA sample (left) and total pore space in our 1H sample (right). Both samples are fully-resolved (not digitally coarsened).

The vertical distribution of porosity of each sample is plotted in Figure 5. For the DA sample, the top is located at 6 cm and the bottom is located at 0 cm, and a few millimeters from both ends were not included in the digital analysis to avoid boundary effects. The connected porosity is always lower than the total porosity, as expected. While there is some fluctuation in porosity with depth, we notice a slight trend of increasing porosity with sample depth. A possible reason for this behavior is the sample was compacted on only one end, namely the top-end. Thus, the porosity is smaller at the top than at the bottom. Furthermore, the typically observed bathtub shape in the porosity-distribution is not very evident in our DA sample, although it is possible that it could appear in the profile if a few more slices were included on the ends. For the 1H sample, the top is located at approximately 4.3 cm and the bottom is located at 0 cm, and a few millimeters from both ends were not included in the analysis, similar to the DA sample. The vertical porosity distribution in the 1H sample is quite different from the DA sample; it is quite non-uniform and contains a sudden reduction of porosity at about 2.3 cm. That is, the top half of the sample has an average porosity of 0.4 while the bottom half has an average of 0.003. This bottom half contains very few pores, and any pore that does exist is very isolated from its surrounding pores. It is unlikely that water would easily filter through this road's top layer, and of course, it was never designed too.

For comparison, the porosity of the DA sample was measured in the lab using the CoreLock apparatus and found to be 16.6%.

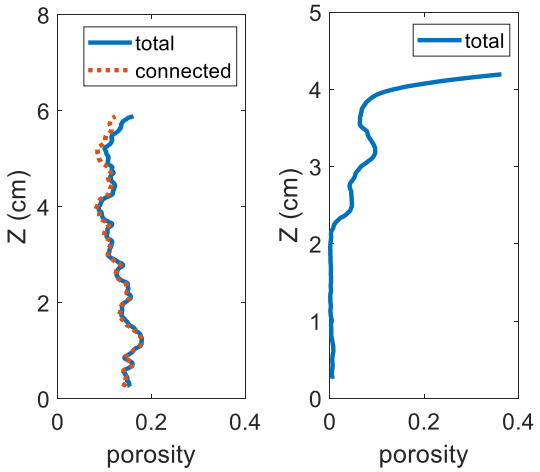

Figure 5: Vertical distribution of porosity in our DA sample (left) and 1H sample (right). Both samples are fully-resolved (not digitally coarsened).

Besides the porosity distributions, we are interested in knowing how fast our detect-connected-pores algorithm is. Our algorithm that detects the top-to-bottom connected pore space is computationally intensive because it uses two different while-loops that must iterate many times until the search for connected cells is over. The first row of Table 3 shows the CPU run time and number of while-loop iterations required in the finest resolution of our DA sample which contained around 218 million pore voxels.

Table 3: CPU run time and while-loop iterations required to detect connected pores in our DA sample in the non-coarsened case (1) and two coarsened cases (15 and 30).

Coarsening level	# pore voxels ($x10^6$)	#connected pore voxels ($x10^6$)	CPU run time (min)	# while-loop its. needed
1	218.05	207.16	1022	5468
15	14.82	13.36	35.7	3360
30	7.56	6.00	17.7	3058

We consider the CPU run time of 1022 minutes problematic. To reduce the amount of time it takes for the detect-connected-pores algorithm to finish, we ran several data coarsening experiments. That is, we coarsened the vertical resolution of the samples, and studied how CPU run time, number of while-loop iterations, total and connected porosity changes with vertical coarsening. Results from the R=15 and R=30 coarsening experiments performed on the DA sample are shown in the rest of Table 3 and the iteration count results from all of the coarsening experiments performed on this sample are plotted in Figure 6.

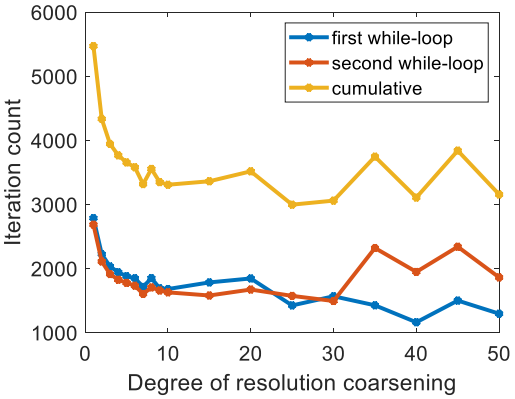

Figure 6: Influence of coarsening on the number of iterations required for the detect-connected-pores algorithm to finish.

Coarsening most certainly reduces the CPU run times, mainly because less while-loop iterations are required before all neighboring-cells to pore-cells have been labelled as NaN (which means they do not get checked again). However, our intention is to maintain sufficient accuracy of the digitally measured porosity values, and thus realize we cannot over-coarsen the datasets. The vertical distributions of porosity under R=1, R=15, and R=30 are shown in Figure 7. These profiles show that coarsening smooths out some of the perturbations in both the total and connected profiles, and that the connected profile moves further to the left of the total profile as the degree of coarsening increases. This means the pore space is less connected as the sample dataset is coarsened. Going back to Figure 6, there is a sudden change in iteration count behavior at around R=30 and above: it is likely that over-coarsening has resulted in a connected pore structure that looks quite different from the previous coarsening degree. Skipping over the key pores that link the majority of the connected pore space together can produce a very different result.

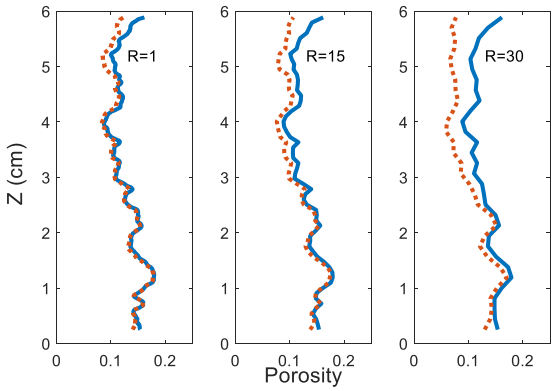

Figure 7: Total (solid line) and connected (dashed line) porosity distribution in the DA sample dataset that was coarsened by various degrees: R = 1, 15, 30.

To better quantify the effect of coarsening, we compare the porosity values in each coarsened sample (R=2 to 50) against the porosity values in the finest-resolved sample (R=1). That is, we calculate the relative difference between coarsened to non-coarsened (or finest) results. Results for the DA sample are presented in Figure 8.

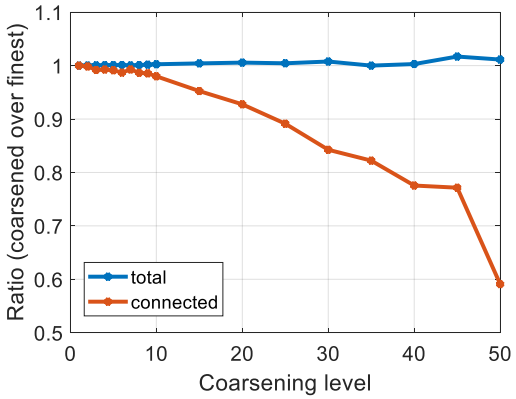

Figure 8: Impact of resolution coarsening on the digitally measured total and connected porosity in the DA sample. Results are given in terms of porosity divided by finest porosity.

This plot indicates the following three things. First, coarsening tends to overestimate total porosity and at the same time underestimate connected porosity. Second, accuracy is not greatly sacrificed under coarsening of R=2 to 10 (up to 0.5% relative difference for total porosity and 2% relative difference for connected porosity; see R=10). But applying coarsening beyond R=10 results in up to

1% relative difference for total porosity and 40% relative difference for connected porosity; see R=50. And third, coarsening impacts the connected porosity measurement more than the total presumably because more pores have become isolated from the top-to-bottom pore pathways. The pores along the perimeter of the cylindrical sample could be most suspectable to isolation.

4. Summary

This work presents an algorithm to detect the connected pore space of porous asphalt. This algorithm was applied on a real porous asphalt sample and the pore space was characterized in terms of its 2D porosity distribution in the vertical direction. The algorithm was assessed in terms of the time it took to analyze the dataset comprised of about 200 million pore cells. To reduce the computational intensity of analyzing 200 million cells, the dataset of the DA sample was vertically coarsened and acceptable estimates of the connected pore space were obtained in a much shorter length of time. Specifically, a coarsening level of 10 cut the CPU time by a factor of around 25 while producing a digital representation that was only 2% difference relative to the full resolution result. The detect-connected-pores code is available online; see link presented in the Author Notes section below. Future work is planned to develop the repository further to include code used to simulate water filtration through the pore space and characterize fluid flow parameters such as permeability and tortuosity, as well as to calculate parameters that include mechanical characteristics of the asphalt such aggregate-to-aggregate contact, binder layer thickness, etc.

Author Notes

The online repository we created for porous asphalt analysis and used in this work is available at: https://github.com/AllenGitCode/PorousAsphalt-ImageProcessing.

Acknowledgment

We thank Statens Vegvesen (The Norwegian Public Roads Administration) for making the asphalt samples used in this work, as well as for performing the laboratory tests on the samples.

We thank NGI (Norwegian Geotechnical Institute) for the use of their CT scanner to obtain the image datasets.

Part of this work was funded by Konnekt (National competence center for transport in Norway) under project code/title: 202640/Collaborative project on transport infrastructure.

References

Aalst, W. van, Derksen, G., Schackmann, P.-P., Paffen, P., Bouman, F., & Ooijen, W. van. (2015). Automated Ravelling Inspection and Maintenance Planning on Porous Asphalt in the Netherlands. International Symposium Non-Destructive Testing in Civil Engineering (NDTCE 2015). Berlin.

Bondt, A., Plug, K., van de Water, J., The, P., & Voskuilen, J. (2016). Development of a durable third generation Porous Asphalt with a high noise reduction. doi: 10.14311/EE.2016.171

Chen, S., You, Z., Yang, S.-L., Garcis, A., Rose, L. (2021) Influence of air void structures on the coefficient of permeability of asphalt mixtures. Powder Technology, 337, 1-9. doi: 10.1016/j.powtec.2020.08.082

De-Ville, S., Menon, M., Jia, X., Reed, G., Stovin, V. (2017) The impact of green roof ageing on substrate characteristics and hydrological performance. Journal of Hydrology, 547, pp. 332-344. doi: 10.1016/j.jhydrol.2017.02.006

Dylla, H., & Hansen, K. R. (2015). Porous asphalt pavements with stone reservoirs.

Ferreira, W.L.G., Branco, T.F.C., Caro, S., Vasconceios, K. (2021) Analysis of water flow in an asphalt pavement surface layer with different thicknesses and different permeability coefficients. Road Materials and Pavement Design, 22(1), 82-100. doi: 10.1080/14680629.2019.1617186

Jagadeesh, A., Ong, G. P., & Su, Y. M. (2022). Selection of image processing algorithms for evaluation of pervious pavement pore network properties. In Road and Airfield Pavement Technology: Proceedings of 12th International Conference on Road and Airfield Pavement Technology, 2021 (pp. 559-571). Cham: Springer International Publishing.

Kassem, A., Linnerud, A.H., Martinussen, T.S. (2023). Digitale tvillinger for kvalitetskontroll av asfaltdekker. Bachelor's thesis, Oslo Metropolitan University.

Król, J. B., Khan, R., Collop, A. C., (2017) The study of the effect of internal structure on permeability of porous asphalt. Road Materials and Pavement Design. doi: 10.1080/14680629.2017.1283355

Plug, K., & Bondt, A. (2021). Maintenance and Rehabilitation OPA8-Inlay as heavy maintenance measure for OPA8 Porous Asphalt.

Roseen, R. M., Ballestero, T. P., Houle, J. J., Briggs, J. F., & Houle, K. M. (2012). Water quality and hydrologic performance of a porous asphalt pavement as a storm-water treatment strategy in a cold climate. Journal of Environmental Engineering, 138(1), 81–89.

Quinteros, V.S., Carraro, J.A.H. (2023) The initial fabric of undisturbed and reconstituted fluvial sand. Geotechnique, 73(1), (pp. 1-15). https://doi.org/10.1680/jgeot.20.P.121

Stanard, C., Candaele, R., Charbeneau, R. J., & Barrett, M. E. (2007). State of the Practice Permeable Friction Courses.

Schuck, B.,Teutsch, T., Alber, S., Ressel, W., Steeb, H., & Ruf, M., (2021) Study of air void topology of asphalt with focus on

air void constrictions – a review and research approach. Road Materials and Pavement Design, 22:sup1, (pp. S425-S443). https://doi.org/10.1080/14680629.2021.1907215

Watson, D., Tran, N. H., Rodezno, C., Taylor, A. J., James, T. M., National Cooperative Highway Research Program, Transportation Research Board, & National Academies of Sciences, Engineering, and Medicine. (2018). Performance-Based Mix Design for Porous Friction Courses (p. 25173). Transportation Research Board. https://doi.org/10.17226/25173